동력시스템공학회지 제28권 제5호 pp. 67-76 2024년 10월 ISSN 2713-8429(Print) ISSN 2713-8437(Online)
Journal of Power System Engineering https://doi.org/10.9726/kspse.2024.28.5.067
Vol. 28, No. 5, pp. 67-76, October 2024

Combustion and Emission Characteristics of Embarked Aircraft Turbine Fuel (JP-5) with Injection Timing Control

Hyungmin Lee*†

(Received 13 August 2024, Revision received 26 September 2024, Accepted 30 September 2024)

Graphical Abstract

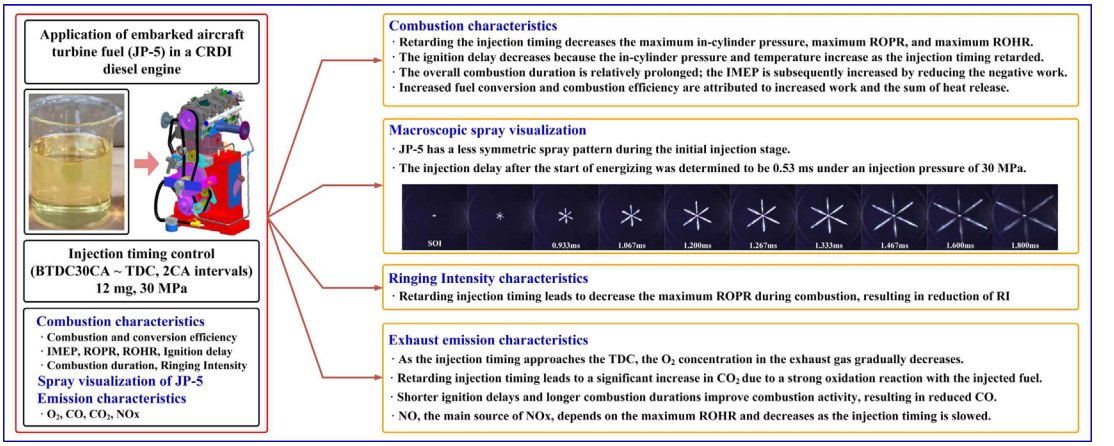

Abstract : This study analyzes the combustion and exhaust emission characteristics with fuel injection timing control by applying JP-5 to a common-rail direct injection diesel engine. JP-5 is supplied to embarked aircraft that are loaded on naval vessels for maritime operational mission. As the fuel injection timing was retarded, the maximum in-cylinder pressure, the maximum rate of pressure rise, and the maximum rate of heat release tended to decrease. As the fuel injection timing approached the TDC, the indicated mean effective pressure and combustion efficiency improved. The ringing intensity, which can be used to quantitatively evaluate the engine noise and vibration level, decreases as the fuel injection timing changes from advanced to retarded. The injection delay period of JP-5 under 30 MPa was approximately 0.53 ms. The spray pattern of JP-5 was less symmetric in the initial stage of injection. The forcible oxidation reaction by retarded fuel injection timing reduces the O_2 concentration in the exhaust gas but increases CO_2 emissions. CO was reduced by oxidation activation, and NO, the main source of NO, decreased with decreasing heat release.

Key Words : JP-5, Combustion, Emission, Spray, Ringing Intensity

— Nomenclature —

ABDC : After bottom dead center
ATDC : After top dead center

*† Hyungmin Lee(https://orcid.org/0000-0003-1999-2604) : Professor, Department of Navigation and Ship Handling System, Republic of Korea Naval Academy.
E-mail : hmsj1226@naver.com, Tel : 051-907-5320

BBDC : Before bottom dead center
BTDC : Before top dead center
CA : Crank angle
CD : Combustion duration
CRDI : Common rail direct injection
EVC : Exhaust valve closing
EVO : Exhaust valve opening
fps : frame per second
ID : Ignition delay
IVO : Intake valve opening
IVC : Intake valve closing
MFB : Mass fraction burned
MPa : Mega Pascal
MW : Mega Watt
TDC : Top dead center
P_{inj} : Injection pressure
rpm : revolution per minute
V_{IVC} : Volume at intake valve closing

1. Introduction

Ground-based military aircraft primarily use JP-8; however, aircraft for maritime operations that are embarked and deployed on naval vessels are supplied with JP-5 fuel. In the late 1980s, North Atlantic Treaty Organization (NATO) nations decided to standardize the fuel used in land-based military aircraft, combat vehicles, and engine-mounted weapon systems to jet propellant (JP)-8 for efficient logistics support. In addition, JP-5 was selected as a fuel to replace JP-8 in emergency situations.[1)]

JP-5 and JP-8 are kerosene-based military aviation fuels, and their density, viscosity, and cetane number are lower than those of diesel fuel. In particular, JP-5, which is stored on naval ships rather than in land-based storage facilities, requires a minimum flash point of 60°C to ensure storage stability.

Naval vessels that deploy maritime operational aircraft store two types of fuel: High-Sulfur Diesel (HSD) fuel used for propulsion and generation of vessels and JP-5, which is supplied to aircraft. Compared with diesel fuel, JP-8 has an asymmetric spray shape, a long ignition delay, and a stronger premixed combustion intensity, which increases Nitrogen Oxide (NOx) emissions.[2,3)]

However, few studies have analyzed various characteristics of JP-5 in diesel engines because the scope of application of naval aircraft turbine fuel is limited to naval vessels. Additionally, in the event of an emergency where diesel fuel cannot be supplied to the propulsion and power generation diesel engines mounted on the naval vessels, JP-5 for embarked aircraft fuel must be used to the diesel engine to enable continuous operating mission. If the single fuel policy of JP-5 is implemented on naval vessels, various combustion and performance experimental research of JP-5 in diesel engines is necessary.

The advantage of a common-rail diesel engine equipped with an electronic injector is that it can improve engine performance and reduce exhaust gas by applying various fuel injection strategies. In a common-rail diesel engine, fuel injection timing control is an attractive fuel injection strategy that plays an important role in the combustion process and exhaust gas formation.[4,5)]

In general, when the fuel injection timing is advanced, the ignition delay increases because of the low in-cylinder pressure and temperature. In addition, controlling the timing of fuel injection has a strong influence on the formation of Carbon Oxide (CO) and NOx.[6)]

This study focused on analyzing the combustion, Ringing Intensity (RI), and emission characteristics, including the spray pattern of JP-5, according to fuel injection timing control by applying JP-5 to a common-rail diesel engine used in an embarked aircraft turbine.

2. Experimental setup and conditions

Fig. 1 shows a schematic of a test device for analyzing the combustion and emission characteristics of turbine fuel with fuel injection timing control in embarked aircraft.

The test device consists of a single-cylinder, common-rail diesel engine that is capable of controlling fuel injection timing (Table 1), a 22 kW electric motor for precise control of engine speed, a portable exhaust emission analyzer, and a visualization system capable of analyzing the spray characteristics of embarked aircraft turbine fuel. The functions of the main components of the test device are summarized in Table 2.

The fuel investigated in this research is JP-5, which is used for embarked aircraft that are loaded onto naval ships to carry out maritime operational missions.

The physiochemical properties of JP-5 and HSD of stored on naval vessels carrying embarked aircraft are compared in Table 3.

The injection strategy applied in this study to analyze the combustion and exhaust emission characteristics of JP-5 is fuel injection timing control.

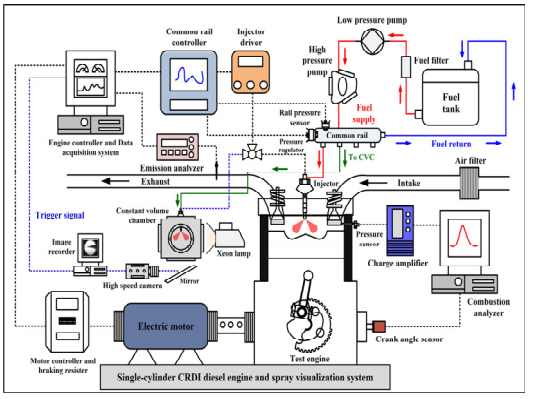

Fig. 1 Schematic of the experimental system

Table 1 Specifications of the test engine

Parameter	Value	
Manufacturer	Mobiltek	
Model	MT-SCDE 100	
Type	CRDI diesel engine	
Number of cylinder	1	
Bore × Stroke	83 mm × 92 mm	
Compression ratio	17.7:1	
Displacement	498 cc	
Valve timing	IVO	BTDC7CA
	IVC	BTDC43CA
	EVO	BBDC52CA
	EVC	ATDC6CA

Table 2 Functions of the key instruments

Instruments	Main function (model)
Electric motor	Precise engine speed control (22 kW, HV2 induction motor)
Injection controller	Fuel injection control with pulse (ZB-5100)
Exhaust gas analyzer	Emission measurement (Testo-350K)
Piezoelectric pressure sensor	In-cylinder pressure measurement (Type-6056A)
Combustion analyzer	Combustion characteristic analysis (MT-7000S)
High speed camera	Fuel spray record (FASTCAM SA2)
Optical lamp	1 kW light source

Table 3 Physiochemical properties of JP-5 and HSD

Properties	Value	
	JP-5	HSD
Carbon (wt %)	85.80	86.97
Hydrogen (wt %)	14.07	12.64
Sulfur (wt %)	0.090	0.038
Density (kg/m^3, 15℃)	801.0	849.4
Kinematic viscosity (mm^2/s)	1.356	3.621
Flash point (℃)	48.2	52.8
Lower heating value (kJ/kg)	42,950	42,710
Distillation temperature (℃)	Illustrated in Fig. 2	

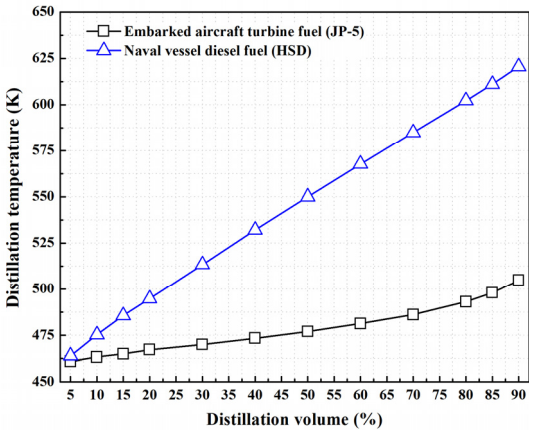

Fig. 2 Distillation temperatures of JP-5 and HSD

The fuel injection timing was adjusted from BTDC30CA to TDC in 2CA intervals, the fuel injection pressure was fixed at 30 MPa, and the engine speed was kept constant at 1,000 rpm for the test.

A visualization system consisting of a high-speed camera and a constant volume chamber was used to analyze the spray characteristics of JP-5, and the fuel was supplied from the common rail of the test engine. Table 4 shows the detailed test conditions.

Table 4 Experimental conditions

Parameter	Value
For engine operating	
Test fuel	JP-5
Engine speed	1,000 rpm
Injection pressure (P_{inj})	30 MPa
Injection mass (m_f)	12 mg
Injection timing	BTDC30CA ~ TDC (2CA intervals)
Coolant temperature	333 K
Intake temperature	Room temperature
Emission sampling	O_2, CO, CO_2, NO
For macroscopic spray visualization	
Injection pressure (P_{inj})	30 MPa
Injection mass (m_f)	12 mg
Ambient pressure (P_{amb})	0.1 MPa
Camera frame rate	15,000 fps (256×256 pixels)
Exposure time	0.04 μs

3. Experimental results and discussion

3.1 Combustion characteristics

Fig. 3 shows the results of the in-cylinder pressure and rate of heat release (ROHR) with fuel injection timing control.

The ROHR is calculated by applying the measured in-cylinder pressure and Equation (1) derived from the first law of thermodynamics.

$$\frac{dQ}{d\theta} = \frac{k}{k-1} P\frac{dV}{d\theta} + \frac{1}{k-1} V\frac{dP}{d\theta} \quad (1)$$

Where $dQ/d\theta$ is the ROHR, k is the specific heat ratio, $dV/d\theta$ is the volume change rate according to the crank angle, and $dP/d\theta$ is the rate of pressure rise (ROPR).

As the fuel injection timing changes from BTDC24CA to TDC, the in-cylinder pressure and ROHR increase and then decrease again. When the fuel injection timing is advanced, the in-cylinder pressure and temperature are low; thus, the ignition

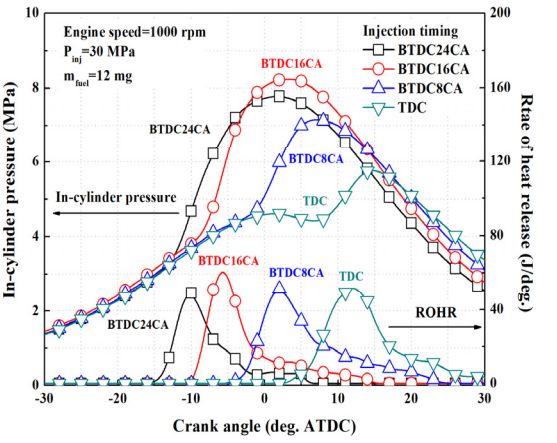

Fig. 3 In-cylinder pressure and ROHR characteristics

delay increases.

Since the combustion of the mixture is temporary, the intensity of the premixed combustion substantially increases, which affects the maximum in-cylinder pressure and the ROHR. As the fuel injection timing changes from the advanced condition to the TDC region, the in-cylinder pressure and temperature increase, causing a decrease in the ignition delay and the premixed combustion intensity. Thus, the maximum in-cylinder pressure and the maximum ROHR decrease.

Fig. 4 shows the results of the maximum in-cylinder pressure, maximum ROPR, and maximum ROHR according to the fuel injection timing control.

On the basis of BTDC18CA ~ BTDC16CA, as the fuel injection timing is changed to an advanced condition, the maximum in-cylinder pressure, maximum ROPR, and maximum ROHR decrease.

As the fuel injection timing is changed toward BTDC30CA, the in-cylinder pressure and temperature dramatically decrease. In particular, since some of the injected fuel flows into the squish and crevice areas, the combustion reaction is not activated. Therefore, the maximum in-cylinder pressure, maximum ROPR, and maximum ROHR decrease.

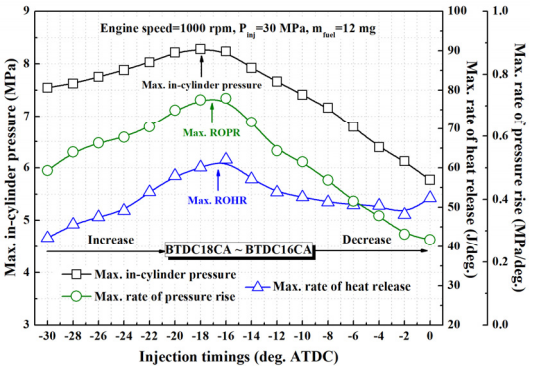

Fig. 4 Max. P, Max. ROPR, and Max. ROHR characteristics

In addition, retarding the injection timing toward TDC via BTDC18CA ~ BTDC16CA results in a shorter ignition delay, which decreases the premixed combustion intensity. The reduced premixed combustion intensity plays a vital role in lowering the maximum in-cylinder pressure, maximum ROPR, and maximum ROHR.

Fig. 5 shows the effects of controlling the fuel injection timing on the ignition delay, combustion duration, and exhaust gas temperature.

As the fuel injection timing is delayed toward the TDC, the in-cylinder pressure and temperature increase. Thus, the ignition delay decreases, and the overall combustion duration is prolonged.

As the combustion duration increases, the exhaust gas temperature increases due to theeffect of post combustion, which reduces the negative work in the compression stroke process, resulting in an increase in the IMEP and an improvement in the combustion efficiency.

Fig. 6 shows the IMEP, fuel conversion and combustion efficiency according to the fuel injection timing control of JP-5. Equations (2) and (3) were applied to derive the results of Fig. 6.

$$IMEP = \frac{\Delta\theta}{V_d} \sum_{i=n_1}^{n_2} P(i) \frac{dV(i)}{d\theta} \tag{2}$$

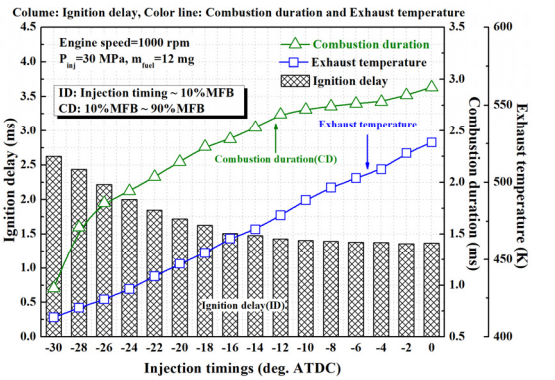

Fig. 5 Ignition delay, combustion duration, and exhaust temperature characteristics

$$\eta_{fc} = \frac{W_{ind}}{m_f Q_{LEV}}, \quad \eta_{comb} = \frac{\sum ROHR}{m_f Q_{LEV}} \tag{3}$$

Where IMEP is the indicated mean effective pressure, V_d is the displacement volume, η_{fc} is the fuel conversion efficiency, η_{comb} is the combustion efficiency, W_{ind} is the indicated work, m_f is the fuel mass, Q_{LEV} is the lower heating value, and $\sum$ROHR is the total ROHR.

The IMEP is a representative index for evaluating combustion performance. The IMEP decreased as the fuel injection timing advanced from TDC to BTDC30CA.

Since most of the heat released by combustion under advanced conditions occurs during the compression stroke and acts as negative work, the IMEP decreases as the fuel injection timing advances. Therefore, the fuel conversion efficiency and combustion efficiency also decrease.

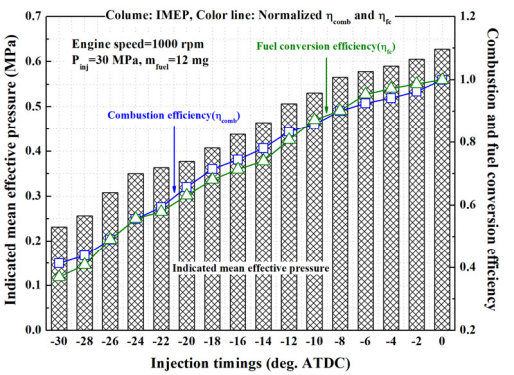

Fig. 6 IMEP, normalized fuel conversion and combustion efficiency characteristics

3.2 Ringing Intensity characteristics

The engine noise and vibration levels vary depending on the fuel injection timing control. A representative theory is needed to quantify the effects of combustion characteristics on engine noise and vibration levels according to fuel injection timing control.

The RI theory, which was introduced to evaluate the knocking phenomenon during the combustion process, is closely related to the acoustic energy of the pressure wave generated during the combustion process and can be used to quantify engine noise and vibration.

The limit value of the RI, which reflects the knocking state depending on the combustion conditions, is 2 MW/m^2 to 6 MW/m^2; however, 5 MW/m^2 is generally adopted. Equation (4) shows the RI calculation formula for quantitatively evaluating engine noise and vibration.[7,8]

$$RI = \frac{\sqrt{kRT_{\max}}}{2kP_{\max}} \left[\beta \left(\frac{dP}{dt}\right)_{\max}\right]^2 \tag{4}$$

Where RI is the ringing intensity, k is the specific heat ratio, R is the universal gas constant, T_{max} is the maximum in-cylinder temperature, P_{max} is the maximum in-cylinder pressure, β is a constant (0.05 ms), and $(dP/dt)_{max}$ is the maximum ROPR expressed by converting the crank angle into time. T_{max} can be calculated via the measured in-cylinder pressure data and Equations (5) to (7).[9,10]

$$T(\theta) = \frac{P(\theta)\, V(\theta) MW_m}{m_{cylinder} R} \tag{5}$$

$$m_{cylinder} = m_{air} + m_{fuel} \tag{6}$$

$$MW_m = \frac{MW_{air} MW_{fuel}[1 + (A/F)_s]}{MW_{air} + MW_{fuel}(A/F)_s} \tag{7}$$

Where $T(\theta)$ is the in-cylinder gas temperature according to the crank angle, MW_m is the sum of the molecular weights of air and fuel, $m_{cylinder}$ is the total mass of air and injected fuel at the intake valve closing, R is the universal gas constant, MW_{air} is the molecular weight of air (28.84 g/mol), MW_{fuel}

is the molecular weight of JP-5 (166 g/mol), and $(A/F)_s$ is the stoichiometric air fuel ratio of JP-5.

Fig. 7 depicts the results of the RI characteristics according to the fuel injection timing control. On the basis of BTDC16CA, the RI tends to decrease as the fuel injection timing advances toward BTDC30CA and is retarded toward TDC. Notably, the RI in Equation (4) is absolutely dominated by the maximum ROPR.

The ROPR also increases in the region where the premixed combustion intensity strongly occurs. Therefore, the strength of the RI, which is under the absolute control of ROPR, is increasing. When the ignition delay period is shorter, the premixed combustion intensity also decreases; thus, the ROPR also decreases.

This acts as a key factor for lowering the RI, and it can be confirmed that slowing the fuel injection timing through RI quantification is an effective strategy for reducing engine noise and vibration.

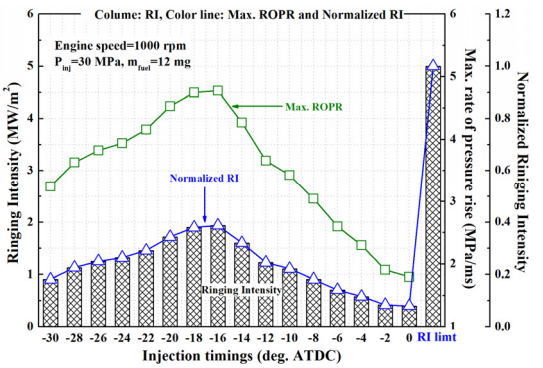

Fig. 7 Ringing Intensity characteristics

3.3 Macroscopic spray characteristics

There are few studies on the macroscopic spray characteristics of JP-5. The JP-5 supplied to maritime aircraft is not much different from the JP-8 used as a land-based aircraft fuel. Fig. 8 shows the definition of spray tip penetration.

Fig. 9 shows the spray development process of JP-5. The start of the high-speed camera shooting was synchronized with the start of energizing (SOE) time of the injector.

The spray pattern shows less symmetric characteristics in the initial injection stage. These spray characteristics are closely related to the internal flow of the injector nozzle. The *Re*, which

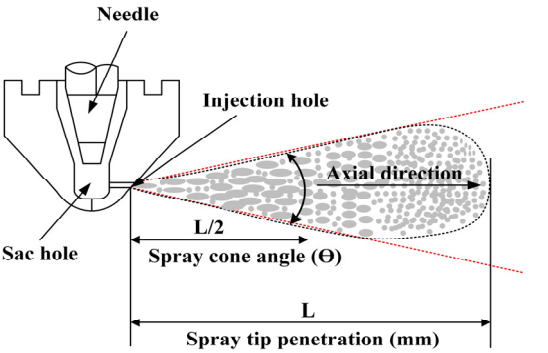

Fig. 8 Spray tip penetration definition11)

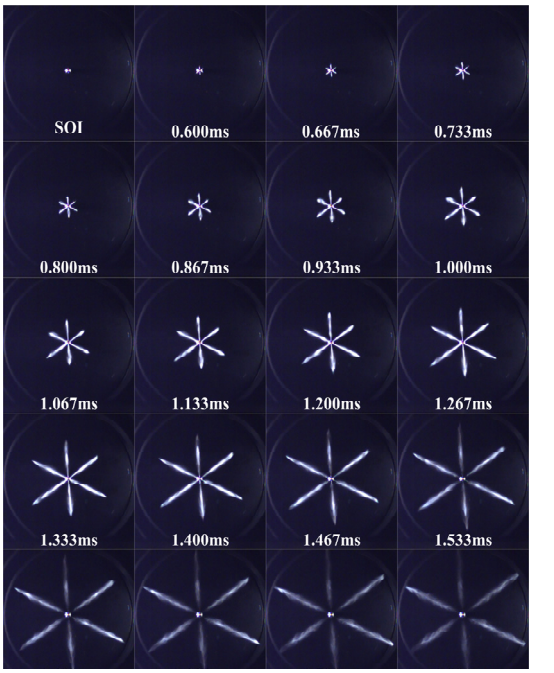

Fig. 9 Spray development process of JP-5

increases when the kinematic viscosity of the fluid is low, is expressed in Equation (8).[12)]

$$Re = \frac{\rho_{fuel} V_{mean} d_o}{\mu} = \frac{V_{mean} d_o}{\nu_{fuel}} \quad (8)$$

Where *Re* is the *Renolds number*, ρ_{fuel} is the density of the fuel, V_{mean} is the injection flow mean velocity, do is the injector nozzle diameter, μ is the absolute viscosity, and ν_{fuel} is the kinematic viscosity of the fuel. The *Re* of JP-8, which has similar properties to those of JP-5, with the exception of the minimum flash point, is approximately 39300 (*Re* is 17700 for diesel fuel).[2)] An increase in *Re* affects the turbulence intensity inside the injector nozzle, and in the case of JP-5 with low kinematic viscosity, the strong turbulence intensity is considered the greatest cause of less symmetric spray.

Fig. 10 shows the spray tip penetration of JP-5, which is expressed by measuring the axial direction in the spray development photograph of Fig. 9.

The fuel injection delay time after the SOE timeis approximately 0.53 ms, and the spray tip penetration increases rapidly after the start of injection (SOI).

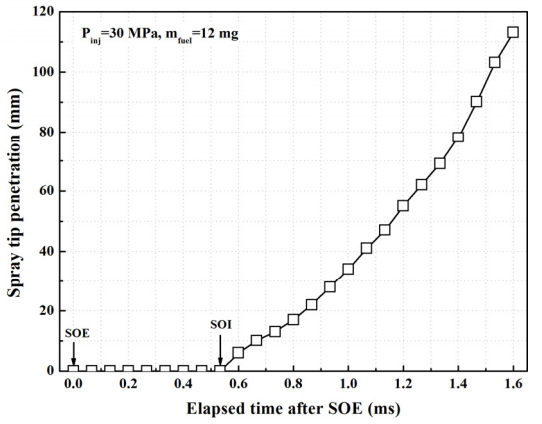

Fig. 10 Spray tip penetration characteristics

3.4 Emission characteristics

Fig. 11 shows the characteristics of O_2 and CO_2 in the exhaust gas according to the fuel injection timing control. As the fuel injection timing is retarded, the concentration of O_2 in the exhaust gas tends to decrease. Retarding the fuel injection timing decreases the ignition delay and increases the combustion duration; thus, the oxidation reaction of the fuel is further promoted.

CO_2 tends to increase as the fuel injection timing is delayed. Retarding the injection timing improves the combustion efficiency and promotes the oxidation reaction of the fuel, which increases the burned rate of the injected fuel. This phenomenon

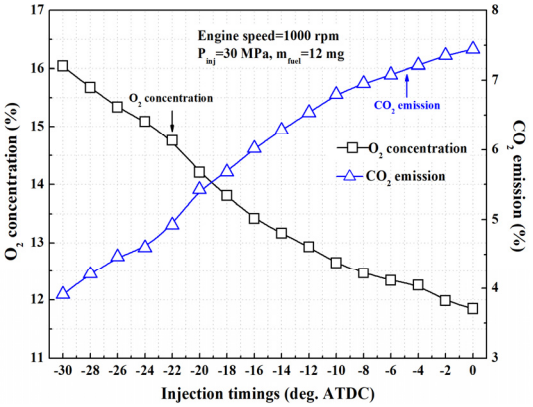

Fig. 11 O_2 and CO_2 characteristics

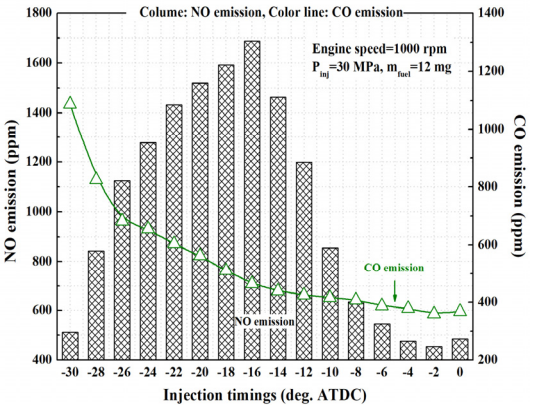

Fig. 12 NO and CO characteristics

caused the increase in CO_2.

Fig. 12 displays the effects of fuel injection timing control on NO and CO emissions.

A significant factor for CO production is incomplete combustion due to insufficient oxidation and cylinder wall wetting under lower in-cylinder pressure and temperature conditions.[13)]

As the fuel injection timing is delayed, the combustion performance is improved, and the oxidation reaction of the fuel is better promoted; thus, CO is reduced because of superior oxidation reaction. NOx is generally composed of NO and NO_2. In contrast to NO_2,

NO is the dominant oxide formed during combustion and is the largest source of NOx emissions.[14)] NO formed during combustion is closely related to heat release rate. As the fuel injection timing changes from advanced to retarded conditions, the maximum ROHR decreases. Thus, NO, the main source of NOx, is reduced because the ignition delay shorts, reducing the premixed combustion intensity and suppressing the heat release.

4. Conclusions

JP-5, which is used as a fuel for naval aircraft, was applied to a single-cylinder common-rail diesel engine equipped with an electronic injector, and the combustion and exhaust emission characteristics were determined with injection timing control. Through analysis of the experimental results, the following conclusions were drawn:

1) The more the fuel injection timing is retarded toward the TDC, the lower the maximum in-cylinder pressure, maximum ROPR, and maximum ROHR are. The short ignition delay and long combustion duration caused by retarding the injection timing increase the IMEP and improve the combustion efficiency.

2) The variable that has the strongest influence on the RI level is the maximum ROPR. The maximum ROPR decreases as the fuel injection timing is retarded, and the RI, which can be used to evaluate the engine noise and vibration level, decreases.

3) JP-5 has a lower kinematic viscosity and higher *Re*, so the strong turbulence formed inside the injector nozzle during fuel injection results in a less symmetric spray pattern in the early stage of injection.

4) As the fuel injection timing is retarded, the oxidation reaction is activated, which reduces the O_2 concentration in the exhaust gas. However, CO_2 emissions increase. As the fuel injection timing advanced, insufficient oxidation and incomplete combustion occur, which increases CO emissions. The emission level of NO, the largest source of NOx products, also decreases as the heat release decreases.

5) In the future research, combustion and emission characteristics from JP-5 in a CRDI diesel engine will be analyzed by applying dynamic injection strategies such as injection pressure, multiple injection and split injection.

Acknowledgement

This research was supported by the 2024 Academic Research Project of the Naval Institute for Ocean Research of the Republic of Korea Naval Academy.

Author contributions

Conceptualization, analysis, writing and review.

References

1. D. M. Korres, D. Karonis, E. Lois, M. B. Linck

and A. K. Gupta, 2008, “Aviation fuel and biodiesel on a diesel engine”, Fuel, 87, 70-78. (https://doi.org/10.1016/j.fuel.2007.04.004)

2. J. Lee and C. Bae, 2011, “Application of JP-8 in a heavy duty diesel engine”, Fuel, 90, 1762-1770. (https://doi.org/10.1016/j.fuel.2011.01.032)
3. C. Bae and J. Kim, 2017, “Alternative fuels for internal combustion engine”, Proceedings of the Combustion Institute, 36, 3389-3413. (http://dx.doi.org/10.1016/j.proci.2016.09.009)
4. H. M. Lee, 2019, “Effects of biodiesel fuel injection timing on combustion, exhaust emissions and energy efficiency in a single diesel engine”, Journal of Power System Engineering, 23(4), 78-83. (http://dx.doi.org/10.9726/kspse.2019.23.4.078)
5. S. G. Cho, 2022, “An effect of injection timing on combustion characteristics of using biodiesel in small fish diesel generator engine”, Journal of Power System Engineering, 26(2), 5-12. (https://doi.org/10.9726/kspse.2021.23.26.005)
6. B. Mohan, W. Yang and S. K. Chou, 2013, “Fuel injection strategies for performance improvement and emissions reduction in compression ignition engines-A review”, Renewable and Sustainable Energy Reviews, 28, 664-676. (http://dx.doi.org/10.1016/j.rser.2013.08.051)
7. J. Dernotte, J. E. Dec and C. Ji, 2014, “Investigation of the source of combustion noise in HCCI engines”, International Journal of Engines, 7(2), 730-761. (https://doi.org/10.4271/2014-01-1272)
8. J. A. Eng, 2002, “Characterization of pressure waves in HCCI combustion”, SAE Technical Paper, 2002-01-2859. (https://doi.org/10.4271/2002-01-2859)
9. N. Septivani and B. W. Riyandwita, 2018, “Spark ignition engine modeling for in-cylinder pressure and temperature prediction using Simulink”, MATEC Web of Conference, 204(04001). (https://doi.org/10.1051/matecconf/201820404001)
10. R. J. Scaringe, 2009, “Extension of the high load limit in the homogeneous charge compression ignition engine”, Ph.D. thesis, Massachusetts Institute of Technology, U.S.A.
11. A. K. Agarwal, V. Kumar, S. Mehra, N. K. Mukherjee, H. Valera and D. Nene, 2023, “Macroscopic and microscopic spray characteristics of dimethyl ether in a constant volume spray chamber using a mechanical fuel injection system for automotive applications”, ASME Open Journal Engineering, 2(0210451), 1-12. (https://doi.org/10.1115/1.4063202)
12. V. L. Streeter, E. B. Wylie and K. W. Bedford, 1998, “Fluid Mechanics”, Mcgraw-Hill, New York, 23-24.
13. S. Imtenam, M. Varman, H. H. Masjuki, M. A. Kalam, H. Sajjad, M. I. Arbab and I. M. Rizwanul Fattash, 2014, “Impact of low temperature combustion attaining strategies on diesel emissions for diesel and biodiesel: A review”, Energy Conversion and Management, 80, 329-356. (https://doi.org/10.1016/j.enconman.2014.01.020)
14. S. Imtenam, S. M. Ashrafur Rahman, H. H. Masjuki, M. Varman and M. A. Kalam, 2015, “Effect of dynamic injection pressure on performance, emission and combustion characteristics of a compression ignition engine”, Renewable and Sustainable Energy Reviews, 52, 1205-1211. (http://dx.doi.org/10.1016/j.rser.2015.07.166)